



RESEARCH ARTICLE - ENGINEERING

Spot Lap Joining of Titanium G2 to Nylon 6 by Nylon Extrusion via Friction Forming Technique

Hashim H. Shareef^{1*}, Ammar A. Hussain¹

¹ Engineering Technical College, Middle Technical University, Baghdad, Iraq.

* Corresponding author E-mail: hashimshareefe@gmail.com

Article Info.	Abstract
<p><i>Article history:</i></p> <p>Received 03 November 2021</p> <p>Accepted 12 December 2021</p> <p>Publishing 31 December 2021</p>	<p>To join sheets of commercial pure titanium grade 2 and nylon 6 polymer, friction lap spot welding (FLSW) was proposed. The titanium sheets were drilled to create a 3.5mm diameter hole, which was then threaded with M4. In this work, the effects of the process parameters on joint quality was investigated. The tool's rotating speed was 710, 900, 1120 RPM, the tool's plunging rate was 0.23, 0.75, 1.3mm/sec, and the tool's diameter was 8,10, and 12 mm. All of the specimens were successfully joined, according to the results. The specimens were fully dislocated from the titanium pre-hole after shearing the polymer at the lap joint region. The Ti-nylon 6 joints had shear forces ranging from 597 to 864N. The axial load measured during the joining operation is found to be 199 kg. The joint shear force was most affected by the rotating speed. The two metals were connected by a mechanical interlock at a micron-wide interface line, according to the microstructure analysis.</p>
<p>This is an open-access article under the CC BY 4.0 license (http://creativecommons.org/licenses/by/4.0/)</p>	
<p>2019 Middle Technical University. All rights reserved</p>	
<p>Keywords: Design of Experiments; Titanium Alloy; Nylon 6; Friction Spot Joining</p>	

1. Introduction

With the rapid advancement of technology in recent years, it has become increasingly important to combine machine components and engineering structures using dissimilar materials. Most applications require unique features not found in a single material, such as high conductivity, hardness, strength, corrosion resistance, and lightweight, among others [1]. It becomes necessary to connect different materials with different properties in order to collect the full benefits of their extra properties. This is especially true in the automotive, aerospace, medical, and biological industries, which rely on innovative materials with specialized properties for great performance while also required lighter structures to save fuel [2]. The development of the automotive industry was aided by titanium and polymer. These materials, on the other hand, are functional, durable, safe, low-maintenance, low-emissions, and enhance fuel efficiency [3]. Titanium is used in a variety of applications, including anode and cathode/cell components, architectural, chemical processing equipment, desalination, air pollution control equipment, navy ship components, sports/recreational equipment, surgical instruments, and watches [4], (Energetics Incorporate, 2017). In contrast, polymers have a significant impact on weight loss and energy efficiency. Ferrous and non-ferrous metals can be replaced by polyvinylchloride (PVC), polyethylene (PE), polypropylene (PP), polystyrene (PS), and other polymers. Polyoxymethylene (POM), polycarbonate (PC), and polyester (Polyester), among others, are engineering plastics with excellent mechanical and thermal resistance. The most of engineering plastics were developed in the 1970s. When compared to engineering plastics, polyphenylene sulfide (PPS), poly-alkyleneisophthalate (PAI), poly-arylate (PAR), polyetherimide (PEI), polyamide (PA), polytetrafluoroethylene (PTFE), and other super engineering plastics have superior mechanical and thermal properties. Polymers used in automobiles include high-performance polymers, light polymers, polymers matrix composite, and sandwich panel polymer [5]. Carbon fiber rain forced polymer (CFRP), a lightweight composite material, is widely used in a variety of industries, including mobility area, automobiles, planes, and other applications. it has a high stiffness, strength, low density, corrosion resistance, and the capacity to absorb energy [6,7]. Welding dissimilar metals presents an unique set of challenges when their physical and mechanical properties are sufficiently different.

Nomenclature			
Ti-G2	Titanium Grade 2	PA6	Polyamide 6
ASTM	American Society for testing and Materials	PA66-GF30	Glass Fiber Reinforced Polyamide
AWS	American Welding Society	PP	polypropylene
FSLW	Friction Spot Lap Welding	PS	polystyrene
RPM	Revolution Per Minute	POM	Polyoxymethylene
CM	Composite Material	PC	Polycarbonate
CFRTP	Carbon Fiber Reinforced Thermoplastic	PE	Polyethylene
DOE	Design of Experiments	PEEK	Poly-ether-ether-ketone
IMCc	Intermetallic Compounds	PEI	Polyetherimide
FLJ	Friction Lap Joining	PET	Polyethylene Terephthalate
FLW	Friction Lap Welding	PVC	Poly Vinyl Chloride
FSLJ	Friction Spot Lap Joining	PAI	poly-alkyleneisophthalate
FSP	Friction Stir Processing	PAR	poly-arylate
FSpJ	Friction Spot Joining	PEI	polyetherimide
FSW	Friction Stir Welding	PTFE	polytetrafluoroethylene
HDPE	High Density Polyethylene	CFRP	Carbon fiber rain forced polymer
HSS	High Speed Steel	PPS	polyphenylene sulfide
NDT	Non-destructive Test	SCF	Short Carbon Reinforced
OM	Optical Microscope	TWI	Technical Welding Institute (of the United Kingdom)

Differences in strength or thermal expansion coefficient can provide high residual stresses, which can lead to cracking. If a filler metal is used, it must be suitable with the base metal [8]. The friction spot welding mechanism was created for this aim, to improve weld properties and prevent metallurgical changes during the welding of various materials [9].

Friction Spot Welding (FSpW) is a solid-state technique for creating a lap-joining area that does not require melting. This technique was more efficient than electric resistance spot welding, TIG spot welding, and Laser spot welding, and it saved large quantities of energy and money. To form a weld region, the FSpW procedure starts with a high-speed rotation of the tool, followed by pressing the tool into the workpiece until the tool shoulder meets the upper workpiece's top surface. Due to the tool's plunging movement, the materials were ejected. The stirring stage begins when the tool reaches a predefined depth after plunging. At this point, the tool is still rotating in the workpiece. Once an acceptable bonding has been achieved, the tool is removed from the workpiece. Porosity, segregation, the formation of brittle intermetallic compounds (IMCs), and heat-affected zone liquid cracking are only a few of the difficulties that the solid-state welding approach addresses in aluminum alloy fusion welding [10]. For polymer-metal structures, the currently available joining technologies (adhesive bonding, mechanical fastening, ultrasonic spot welding, induction welding, injection clinching joining, friction riveting, and laser heating) are often application-specific and have limiting performance properties. This paper studies the effects of joining process parameters (rotating speed, plunging rate and tool diameter) on the joint quality.

2. The Process Details

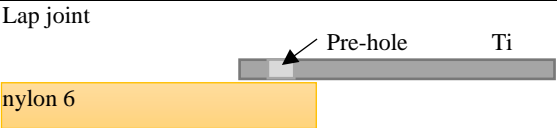
2.1. Materials and dimensions

The welding procedure employed commercial pure titanium g2 and nylon 6 as metal and polymer. Table I shows the mechanical characteristics of titanium and nylon 6. Titanium g2 has a melting temperature of 1669°C [11], for nylon 6 melting the temperature is 240°C [12]. Titanium and nylon 6 specimens were made from two sheets of 1- and 6-mm thickness, respectively. As shown in table 2 and figure 2, each specimen was manufactured with dimensions of 25 x 100 mm² in accordance with the American Welding Society's standard specification of a lap joint area of 25 x 25 mm² (AWS C1.1 M/C1.1:2012). The titanium specimen was placed over the nylon 6 specimen during the welding process, which was accomplished using a lap joint design. In the steel specimen, a single internal M4 thread was used to provide a 3.5 mm hole diameter as shown in fig. 1 & 2.

Table 1 The mechanical properties of titanium and nylon 6

Materials	Yield strength (MPa)	Tensile strength (MPa)	Young modulus (GPa)
Titanium (Grad-2)	219	329	113
Nylon 6	12	46.3	0.32

Table 2 Joint details

Joint feature	Details		
Joint configuration			
Material to be joined	Titanium-grade 2 to nylon 6		
Specimen dimensions (mm)	Metal	Dimension	thickness
	Ti	100×25	1
	Nylon 6	100×25	6

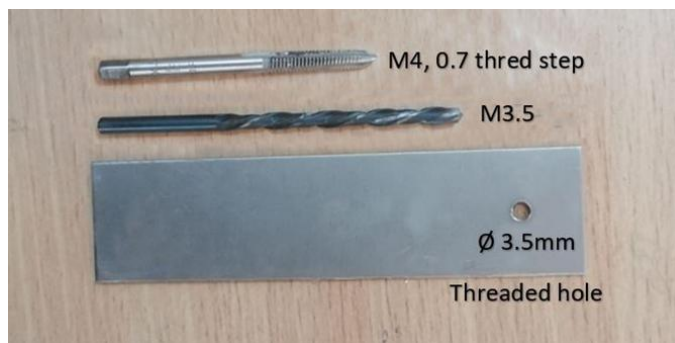


Fig. 1 Threaded hole details of titanium



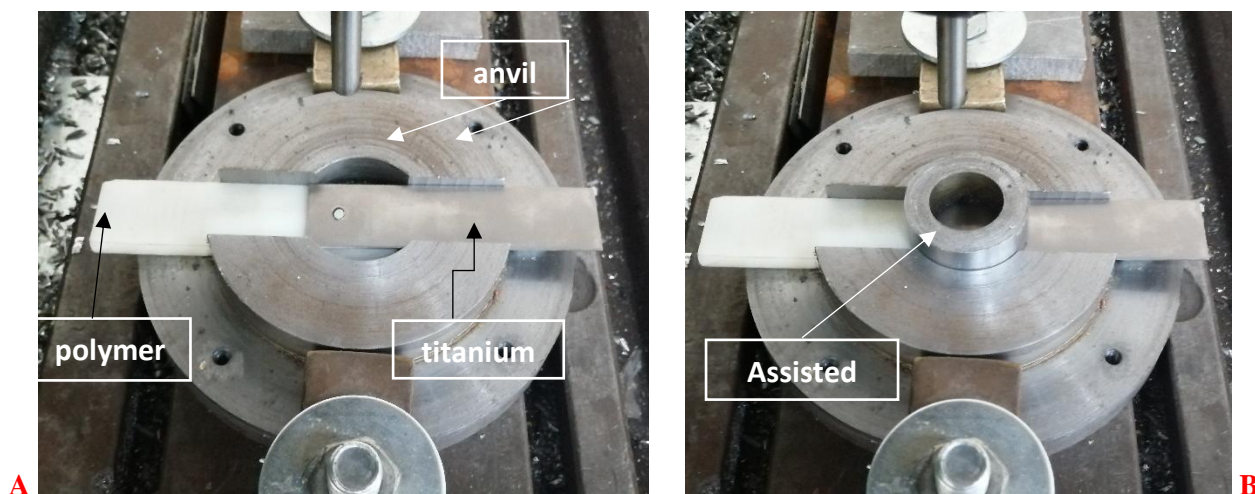
Fig. 2 Titanium and nylon 6 specimens' dimensions

2.2. The Joining Principle

The joining procedure was divided into 3 steps, as follows:

1. Friction the titanium sheet with a rotary tool using the FSpW technique, which generates heat in the friction region and around it.
2. As a result of the preceding operation, the polymer melts in the area beneath the titanium specimen's hole.
3. Using a pin-less tool to push the molten polymer through the hole.

As shown in Fig. 3, the joining procedure was accomplished utilizing the friction spot technique and a vertical milling machine. For the joining procedure, a three-cylinder high-speed steel pin-less tool with shoulder sizes of 8, 10, and 12 mm was developed and used. During the joining procedure, the titanium sheet was positioned on top of the nylon 6 sheet in an overlap arrangement. First, the rotating tool was moved downward until it made contact with the titanium surface. Rotational friction between the upper surface of the titanium specimen and the lower surface of the rotating tool heats the titanium metal in this step. The generated temperature melts the nylon substance, which flows upward toward the titanium hole under the applied force of the rotating tool. Fig. 4 illustrates graphical representations of the steps in the joining process.



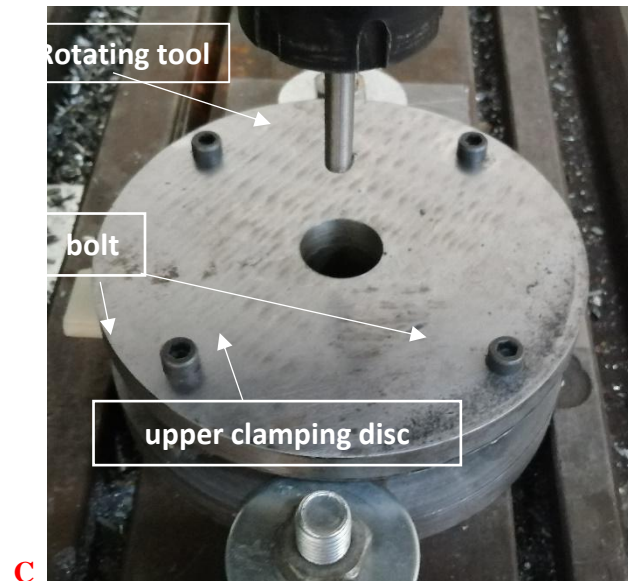


Fig. 3 Stages of sample fixing

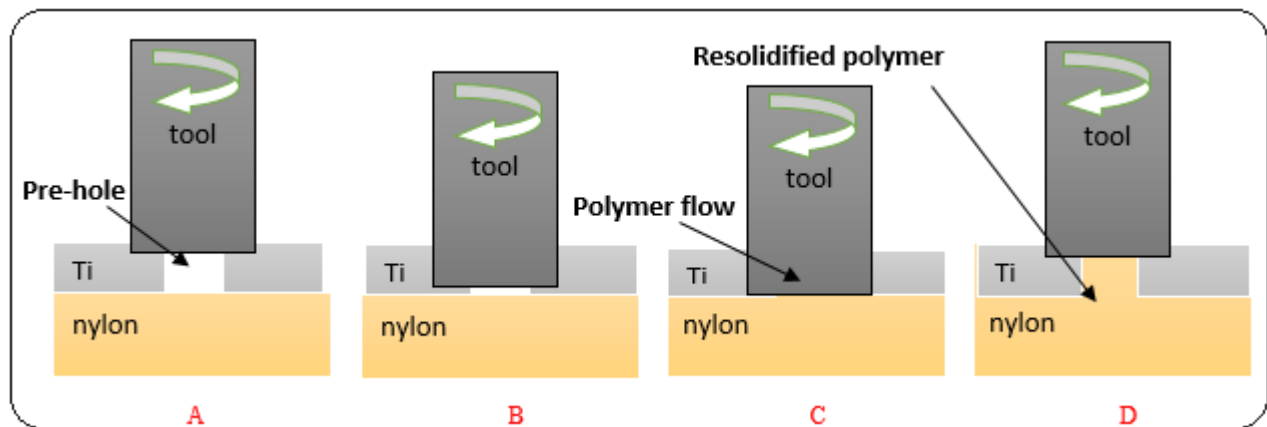


Fig. 4 Graphical illustrations of the joining process steps; (A) before stirring process, (B) contact the rotational tool with titanium and start stirring and heating, (C) heating the polymer and flowing through the hole, (D) removing the tool and the polymer full filling the hole

2.3. Design of the joining parameters experiments

The quality of the joint is influenced by the major process factors (rotation speed, plunging rate, and tool diameter). Because of its effect on joint efficiency, heat generation, and other factors, the FSpJ parameters must be carefully set. With the use of Taguchi design and the MINITAB application, the process parameters were chosen based on the design of the experimental technique (DOE), Three values were used for each parameter. The process parameters group's levels are designed and listed in table 3.

Table 3 Taguchi design of the joining process parameters

No.	Rotating Speed (RPM)	Plunging rate (mm/sec)	Tool Diameter (mm)
1	710	0.23	8
2	710	0.75	10
3	710	1.3	12
4	900	0.23	10
5	900	0.75	12
6	900	1.3	8
7	1120	0.23	12
8	1120	0.75	8
9	1120	1.3	10



Fig. 5 Top view of specimens joining of pre-threaded Ti-g2 to nylon 6

3. Results and Discussion

3.1. tensile Shear force of joints

A tensile test was performed on samples that had been joined according to the joining procedure parameters listed in Table 3, show figure 5. By shearing the extruded polymer in the intermediate zone between the two components, all of the samples failed. The extruded polymer was assumed to have fully entered the titanium hole on the upper surface, representing the circular hole area with a diameter of 3.5 mm in the tensile shear force area. Figure 6 shows the results of the tensile shear force testing for each sample with the various parameter values. The examined samples had tensile shear forces ranging from 597 to 864 N.

Fig. 6 shows the average tensile shear test results that were recorded. Sample 7 has the highest tensile shearing stress while sample 9 has the smallest one, according to that speciality, these two samples were focused-on in the study. To join sample 7, the following process settings were used: 12 mm tool diameter, 1120 rpm rotating speed, 0.23 mm/sec plunging rate the following process parameters were used to join Sample 9: 1120 rpm rotational speed, 0.23 mm plunging rate, and a 10 mm tool diameter. This means that sample 7 was joined at the lowest plunging rate and with the largest tool diameter, whereas sample 9 was joined at the highest plunging rate and with the smallest tool diameter. Both samples were joined at the same rotational speed. As a result, decreasing the plunging rate at the maximum tool diameter of 12mm tends to increase the joint's shear force.

The authors in [13] used joint aluminum with PVC by FSpW method and the parameters used in their work are similar to ours. As their recorded results for 710, 900 and 1120 RPM were 704, 768 and 896 (N), respectively, that was approximately convergent to our results.

Fig. 7 shows the main effect plot of the process parameters on the joint's shear force. It demonstrates that the rotational speed has a minor influence on the joint's shear force, the plunging rate has a larger effect on the joint's shear force at (0.23mm/s), and the shear force reduces as the plunging rate is increased to (0.75mm/s) and then slowly increased at (1.3mm/s). The tool diameter had a moderate effect on the joint's shear force (8mm) and had the lowest and highest shear forces (10,12) respectively.

Fig. 8 presents The Pareto chart showing the effect level of the process parameters on the shear force of the joints showed that C (tool diameter (mm)) had the highest effect on joint shear force, followed by B (plunging rate (mm/sec)), and finally A (rotation speed (rpm)) had the least effect on joint shear force.

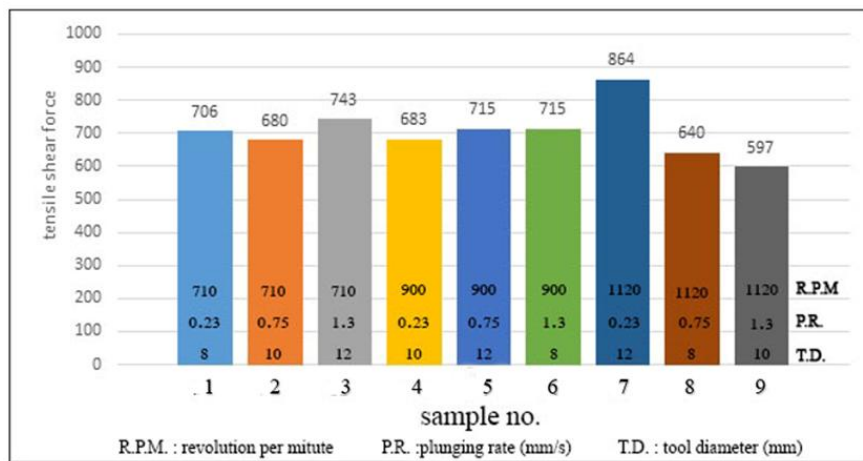


Fig. 6 Variation of the experimental shear forces with process parameters

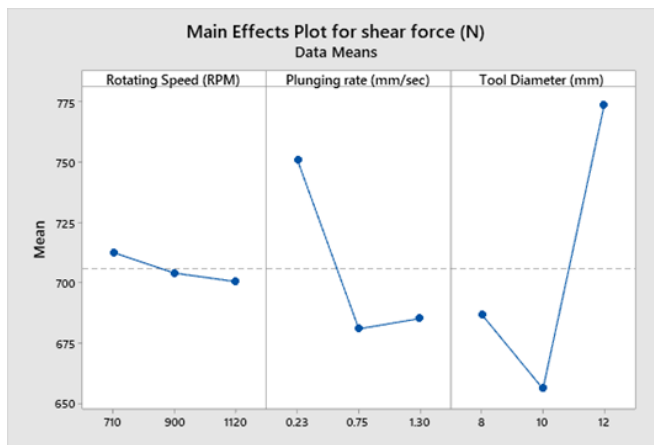


Fig. 7 The main effect plot of joints shear force; pre-hole titanium to nylon 6

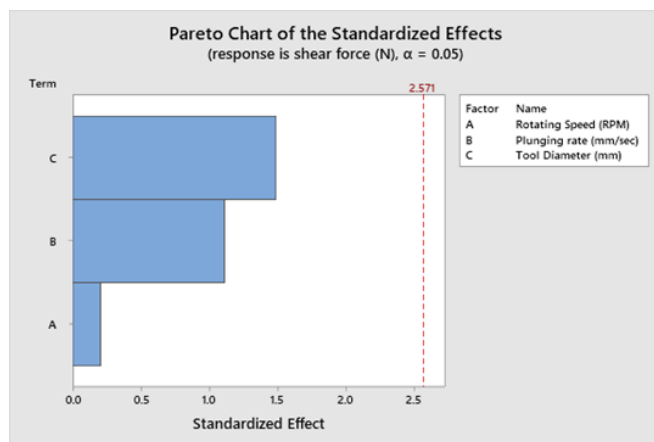


Fig. 8 The Pareto chart of joints shear force

3.2. Fracture features

Table 4 shows the upper and inner surfaces of the weld samples for threaded pre-holed titanium to polymer joints in the fractured zone. Fractures occurred at the interlock area between titanium and polymer, where a pre-hole existed, at all joints of specimens. The surfaces of the joined samples before shear force testing are represented in the first column from the right, the fractured surfaces of titanium and polymer are represented by the other three columns. The first column shows photos of the rotating tool tracing the upper surface of the titanium specimen during the process under the influence of applied pressure and frictional heat between the rotating tool and the titanium surface. All images in the first column of the table show a fully extruded polymer in the holes, while the second and third columns show the upper and inner surfaces of titanium. After the shear force test, the polymer was fully dislocated from the titanium pre-hole and remained with the polymer's base metal without significant deforms on the pre-hole shape, which is attributed to the polymer's high cohesion force and ductility. The extruded circular trace in titanium sheet is clearly visible in the third column, which shows the inner surface of titanium, and this trace extrusion is caused by the applied load and frictional heat of rotating tools. In the fourth column, the extruded circular trace of titanium sheet with heat and axial force forms a stamp-like shape in the polymer zone.




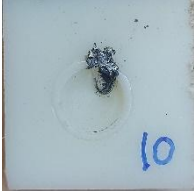







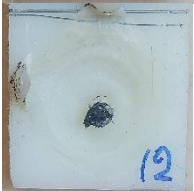




















Fig. 9 shows the upper surface of the titanium specimen before tensile test, a tool trace with a circular form was visible. The presence of molten polymer in the holes is caused by the action of heat (which is generated by friction) as well as the applied load in this process. In the tool trace region of the most of joint samples, there are degradation polymer shown in tool trace and around it as a black particle. This phenomenon of degradation polymer is caused by excessive penetration of molten polymer from the titanium hole and that molten polymer enters the friction process region between the rotational tool and titanium sheet, and because the temperature (that is generating in this region) is higher than the molten temperature of polymer and the applied load. Small titanium chip particles can be seen at and around the tool trace.

3.3. Microstructure features

The microstructure of the composite materials (re-mollified polymer with Ti fragments) inside and outside the hole of the aluminium specimen is shown in Fig. 10 (1-b). Through the cross-sections of the joint holes, the Ti fragments were clearly seen to be distributed in varied sizes from the titanium slag and entrapped in the resolidified layer of the polymer Fig. 10(1-b, 2-1, 2-b). The interface line between the polymers and the titanium hole surface demonstrated the mechanical connection between the titanium pores and the polymer. Furthermore, voids in the nylon 6 were identified, show Fig. 10(1-b), generating a joint weakness and reducing the mechanical properties of the titanium - nylon 6 joints.

Furthermore, an irregular re-solidification zone was found in titanium - nylon 6 joints due to the existence of defects such as voids, which was distributed in an irregular shape Fig. 10(1-b). Those voids created in the hole and beneath the contact between Ti alloy and polymer during the connecting technique. Finally, at the joint zone and inside the joint holes, structural characteristics exhibited a considerable number of macro and micro mechanical interlocks between the Ti- fragments and the melted/re-solidified polymer matrix show Fig. 10(1-b, 2-1, 2-b).

Table 3 Fracture feature of samples

No.	Before shear force test		After shear force test	
	Upper surface of titanium	Upper surface of titanium	Fracture surface of titanium	Inner surface of polymer
1				
2				
3				
4				
5				
6				
7				
8				

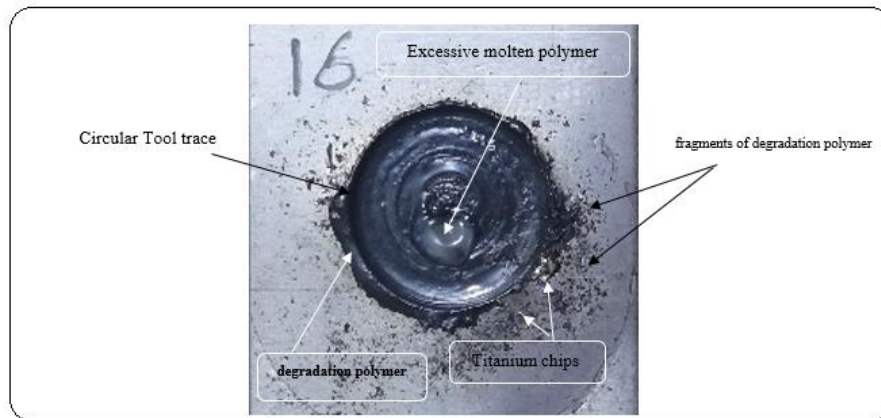


Fig. 9 The upper surface of sample 7 before tensile test

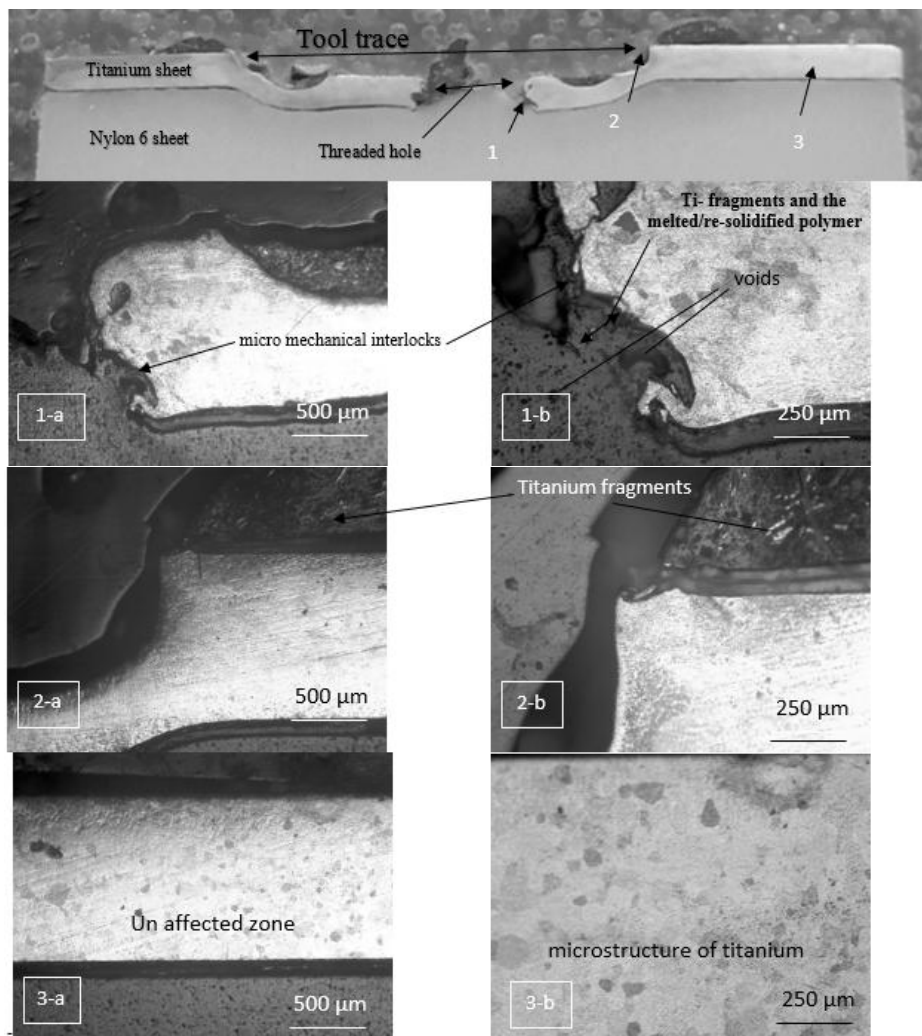


Fig. 10 Microstructure of sample 7 which had the maximum tensile shear force

4. Conclusions

To join titanium alloy g2 and polymer (nylon 6) using a rotating tool to produce the necessary heat to molten the polymer and enter it through the titanium specimen hole, a friction lap spot joining approach was adopted. The impact of hole shape, tool rotational speed, plunge rate, and tool diameter on joint quality was investigated. The following are the main results and observations:

1. All of the samples were successfully connected.
2. A mechanical interlock and partial adhesive connection between the metal and the polymer developed by melting the polymer and penetrating it through the aluminium hole surface.
3. The joint strength was reduced due to the formation of bubbles and a gap between the reaction layers and the resolidified polymer inside the hole.
4. At a rotation speed of 1120RPM, a plunging rate of 0.23mm/sec, a tool diameter of 12mm, and an axial load of 199 kg, the greatest average shear force of the attached sample was found with a value of 864N.
5. The tool diameter had the greatest impact on the joint's shear force.
6. The interface line's width was measured in microns.
7. The specimens were fully dislocated from the titanium pre-hole after shearing the polymer at the lap joint region.

Acknowledgement

I would like to thank the head of applied mechanic Engineering department as well as all the teaching staff for their assistance.

References

- [1] P. Kah, R. Suoranta, J. Martikainen, and C. J. R. o. A. M. S. Magnus, "Techniques for Joining Dissimilar Materials: Metals and Polymers," vol. 36, no. 2, 2014.
- [2] C. Magnus, "Feasibility study of metal to polymer hybrid joining," 2012.
- [3] S. Akinlabi, O. Ogbonna, P. Mashinini, A. Adediran, O. Fatoba, and E. T. Akinlabi, "Titanium and epoxy for automobile application: a review," 2019.
- [4] A. Oryshchenko, I. Gorynin, V. Leonov, A. Kudryavtsev, V. Mikhailov, and E. J. I. M. A. R. Chudakov, "Marine titanium alloys: present and future," vol. 6, no. 6, pp. 571-579, 2015.
- [5] M.-Y. Lyu, T. G. J. I. j. o. p. e. Choi, and manufacturing, "Research trends in polymer materials for use in lightweight vehicles," vol. 16, no. 1, pp. 213-220, 2015.
- [6] A. Katunin, K. Krukiewicz, R. Turczyn, P. Sul, and M. Bilewicz, "Electrically conductive carbon fibre-reinforced composite for aircraft lightning strike protection," in IOP Conference Series: Materials Science and Engineering, 2017, vol. 201, no. 1, p. 012008: IOP Publishing.
- [7] G. Artner, R. Langwieser, R. Zemann, and C. F. Mecklenbräuker, "Carbon fiber reinforced polymer integrated antenna module," in 2016 IEEE-APS Topical Conference on Antennas and Propagation in Wireless Communications (APWC), 2016, pp. 59-62: IEEE.
- [8] M. P. Groover, *Fundamentals of modern manufacturing: materials, processes, and systems*. John Wiley & Sons, 2020.
- [9] S. K. Hussein, I. T. Abdullah, A. K. J. M. M. i. M. Hussein, and Structures, "Spot lap joining of AA5052 to AISI 1006 by aluminium extrusion via friction forming technique," 2019.
- [10] X. W. Yang, T. Fu, and W. Y. Li, "Friction Stir Spot Welding: A Review on Joint Macro- and Microstructure, Property, and Process Modelling," *Advances in Materials Science and Engineering*, vol. 2014, pp. 1-11, 2014.
- [11] E. Gariboldi and B. J. J. o. M. P. T. Previtali, "High tolerance plasma arc cutting of commercially pure titanium," vol. 160, no. 1, pp. 77-89, 2005.
- [12] M. Raheel, *Modern textile characterization methods*. Routledge, 2017.
- [13] F. Y. Sadkhan, S. K. Hussain, and A. H. Khuder, "Friction Spot Joining (FSpJ) process of Aluminium AA6061-T6/Poly Vinly Chloride (PVC)," in IOP Conference Series: Materials Science and Engineering, 2021, vol. 1105, no. 1, p. 012043: IOP Publishing.